2018

On Covariance Matrix Based Spectrum Sensing Over Frequency-Selective Channels

Ming Jin
Ningbo University, mjin@uow.edu.au

Qinghua Guo
University of Wollongong, qguo@uow.edu.au

Youming Li
Ningbo University

On Covariance Matrix Based Spectrum Sensing Over Frequency-Selective Channels

Abstract

This paper concerns covariance matrix based spectrum sensing over frequency selective channels. The impact of frequency selective channels on the covariance matrix of received signals is analyzed in frequency domain and it is shown that the phases of channel spectra degrade the performance of covariance matrix based detectors. To overcome this problem, we propose a new detector which employs only the magnitude spectra of received signals and thereby achieves considerable performance gain. Theoretical performance, in terms of the false-alarm and detection probabilities of the proposed detector, is analyzed. Simulation results verify our theoretical analyses and demonstrate the superior performance of the proposed detector.

Disciplines

Engineering | Science and Technology Studies

Publication Details

On Covariance Matrix Based Spectrum Sensing Over Frequency-Selective Channels

MING JIN [1], (Member, IEEE), QINGHUA GUO [2], (Member, IEEE), AND YOUMING LI[1]

[1]Faculty of Electrical Engineering and Computer Science, Ningbo University, Ningbo 315211, China
[2]School of Electrical, Computer and Telecommunications Engineering, University of Wollongong, Wollongong, NSW 2522, Australia

Corresponding author: Ming Jin (jinming@nbu.edu.cn)

ABSTRACT This paper concerns covariance matrix-based spectrum sensing over frequency-selective channels. The impact of frequency-selective channels on the covariance matrix of received signals is analyzed in frequency domain, and it is shown that the phases of channel spectra degrade the performance of covariance matrix-based detectors. To overcome this problem, we propose a new detector which employs only the magnitude spectra of received signals and therefore achieves considerable performance gain. Theoretical performance, in terms of the false-alarm and detection probabilities of the proposed detector, is analyzed. Simulation results verify our theoretical analyses and demonstrate the superior performance of the proposed detector.

INDEX TERMS Cognitive radio, frequency-selective channels, spectrum sensing, uncalibrated receivers.

I. INTRODUCTION

Cognitive radio, which allows the operation of secondary users (SUs) in the occasionally unused spectrum licensed to primary users (PUs), has been recognized as one of promising technologies for alleviating the problem of spectrum shortage. To probe available spectrum holes and avoid interfering PUs harmfully, spectrum sensing plays a very important role in cognitive radio [1]–[4].

A variety of spectrum sensing methods have been proposed in the literature [3] and [4]. Among the detectors with low computational complexity, energy detection (ED) delivers an outstanding performance without requiring the *a priori* knowledge of primary signals [5]. However, ED needs the knowledge of noise power and its performance degrades severely under noise (power) uncertainty [6]. To combat the noise uncertainty, detection approaches with noise power estimation have been investigated [6]–[9]. In [7], the noise power is initially estimated by switching off radio frequency (RF) terminals, and it is then updated with noise samples from previous sensing durations. However, switching off RF terminals excludes noises from these terminals and surrounding environments. Without disconnecting RF terminals, we proposed two noise power estimators by exploiting the correlations of pilot and cyclic prefix in sensing orthogonal frequency division multiplexing signals

in [8] and [9]. However, the requirement of the *a priori* knowledge about the correlations of primary signals may limit their applications.

To circumvent the requirement of noise power, multiple antennas can be employed for spectrum sensing by exploiting spatial correlations [4]. The eigenvalue-based detection [10]–[14] and the covariance-based detection [15]–[19] are two kinds of typical spectrum sensing methods with multiple antennas. Various eigenvalue-based detectors, such as the maximum-minimum eigenvalue detector (MMED) [11], the maximum eigenvalue to arithmetic mean (MEAM) [12], the arithmetic to geometric mean (AGM) [21], were proposed in the framework of generalized likelihood ratio test (GLRT). In [11], approximate and exact threshold expressions for MMED were presented. In [20], the asymptotic performance of MEAM was analyzed by using the Chi-squared distribution. In [22], the theoretical analysis of AGM (a.k.a. the spherical test) was provided. It can be found that the essential idea behind the eigenvalue-based detectors is in distinguishing whether the popular covariance matrix of received signals is a scaled identity matrix or not. This implies an assumption that the noise variances are the same at all antennas. However, this assumption may not be valid in some scenarios, e.g., the noise variances at different antennas cannot be identical

due to uncalibrated receivers or heterogeneous surrounding environments.

Given sufficiently high spatial correlation, the covariance matrix based detectors work well no matter whether the noise variances of the antennas are identical or not. In [16], we analyzed the theoretical performance of the covariance-absolute value (CAV) detector. In [17] and [18], two weighted versions of the CAV were proposed. In [19], Hadamard ratio detector (HRD) was proposed that exploits the covariance matrix of received signals in frequency domain. However, we will show that the correlation of the received signals from different antennas can decrease considerably due to multi-path propagation (leading to frequency-selective channels). Therefore, the performance of the covariance matrix based detectors will suffer from severe performance loss under frequency-selective channels.

It is shown in this paper that the correlations among the antennas is degraded significantly due to the phases of frequency-selective channel spectra, which motivates the design of a new detector by using only the magnitude spectra of received signals but discarding their phase components. Moreover, comprehensive performance analyses of the proposed detector are provided, and the false-alarm probability (P_f) and detection probability (P_d) are derived. Numerical simulations are provided to validate the theoretical results and demonstrate the superior performance of the proposed detector.

The rest of this paper is organized as follows. After presenting the signal model in Section II, we analyze the effect of multipath propagation on the covariance matrix and propose a new detector based on estimated magnitude spectra of received signals in Section III. In Section IV, the theoretical performance of the proposed detector is analyzed. Simulation results are provided in Section V, followed by conclusions in Section VI.

II. SIGNAL MODEL

Spectrum sensing is usually treated as a binary hypothesis testing problem, i.e., a decision needs to be made on whether primary signals are present or not. We use $\mathcal{H}_0$ and $\mathcal{H}_1$ to represent the null hypothesis (absence of primary signals) and the alternative hypothesis (presence of primary signals), respectively. We assume that at most one primary user operates in a licensed channel and a secondary user is equipped with M antennas. Let $\mathbf{x}_t(n) \in \mathcal{C}^{M \times 1}$, $n = 0, \cdots, N - 1$, denote the discrete-time complex baseband signal vector from the antennas at time instant n, and the mth element of $\mathbf{x}_t(n)$, denoted by $x_{t,m}(n)$, is the signal from the mth antenna. Based on the above binary hypotheses, $x_{t,m}(n)$ can be expressed as

$$x_{t,m}(n) = \eta h_{t,m}(n) \otimes s_t(n - \tau_m) + w_{t,m}(n) \tag{1}$$

where $\otimes$ denotes the convolution operator; η indicates the presence of the primary signal $s_t(n)$, i.e., $\eta = 0$ under $\mathcal{H}_0$ and $\eta = 1$ under $\mathcal{H}_1$, respectively; $h_{t,m}(n)$ represents the channel response between the primary user and the mth antenna of the

secondary user; $w_{t,m}(n)$ denotes the noise at the mth antenna of the SU; τ_m denotes the time delay from the primary user to the mth antenna. Note that the time delays may be different when the antennas are widely spaced to combat the shadowing effect [23]. It is assumed that the channel coefficients keep unchanged within a sensing duration but vary independently among sensing durations, and the channel coefficients of different taps within a sensing duration are independent of each other. The primary signal $s_t(n)$ is assumed to be wide-sense stationary with mean zero and variance σ_s^2. The noise $w_{t,m}(n)$ is also assumed to be wide-sense stationary with mean zero and variance $\sigma_{w,m}^2$, and the noises from different antennas are independent of each other. Note that we have not made any assumption on the distributions of the noise and the primary signal, i.e., they can be non-Gaussian.

By stacking the received signals $\{x_{t,m}(n), \forall m\}$ and absorbing the time delays $\{\tau_m, \forall m\}$ into the channel responses, we can obtain a received signal vector as

$$\mathbf{x}_t(n) = \eta \mathbf{h}_t(n) \otimes s_t(n) + \mathbf{w}_t(n) \tag{2}$$

where

$$\mathbf{h}_t(n) = [h_{t,1}(n - \tau_1), \cdots, h_{t,M}(n - \tau_M)]^T \tag{3}$$

and

$$\mathbf{w}_t(n) = [w_{t,1}(n), \cdots, w_{t,M}(n)]^T \tag{4}$$

with the superscript $(\cdot)^T$ being the transpose operator. With a sufficiently large N and by performing N point Fourier transform on rectangularly windowed sets of N samples, the received signal in frequency domain can be expressed as [24]

$$\mathbf{x}_f(k) = \sum_{n=0}^{N-1} \mathbf{x}_t(n) e^{-j2\pi nk/N}$$
$$\approx \eta \mathbf{h}_f(k) s_f(k) + \mathbf{w}_f(k) \tag{5}$$

where $\mathbf{x}_f(k)$, $\mathbf{h}_f(k)$, $s_f(k)$ and $\mathbf{w}_f(k)$ are the Fourier transforms of $\mathbf{x}_t(n)$, $\mathbf{h}_t(n)$, $s_t(n)$ and $\mathbf{w}_t(n)$, respectively. Note that the index k in $\mathbf{x}_f(k)$ indicates the kth frequency bin, and the coefficient $\mathbf{h}_f(k)$ represents the vector of complex channel coefficients for the kth frequency bin [24].

As $s_t(n)$ and $\mathbf{w}_t(n)$ are wide-sense stationary, according to the central limit theorem (CLT), $s_f(k)$ and $\mathbf{w}_f(k)$ approximately follow Gaussian distributions. This alleviates the requirement of Gaussian distribution of primary signals and noises in time domain. It is not hard to show that

$$s_f(k) \sim \mathcal{CN}(0, N\sigma_s^2) \tag{6}$$

and

$$\mathbf{w}_f(k) \sim \mathcal{CN}(\mathbf{0}, N\mathbf{R_w}) \tag{7}$$

where

$$\mathbf{R_w} = \mathrm{diag}\left\{\sigma_{w,1}^2, \cdots, \sigma_{w,M}^2\right\}. \tag{8}$$

Hence,

$$\mathbf{h}_f(k) s_f(k) \sim \mathcal{CN}\left(\mathbf{0}, N\sigma_s^2 \mathbf{R}_{\mathbf{h}_f}(k)\right) \tag{9}$$

where

$$\mathbf{R}_{\mathbf{h}_f}(n) = \mathbf{h}_f(k)\mathbf{h}_f^H(k) \tag{10}$$

with the superscript $(\cdot)^H$ being the conjugate transpose operator.

III. PROPOSED DETECTOR

In this section, we first investigate the effect of frequency-selective channels on the off-diagonal elements of covariance matrices. We will show that frequency-selective channels make the off-diagonal elements of the covariance matrices under $\mathcal{H}_1$ close to zero, thereby degrading the performance of the covariance matrix based detectors significantly. To remedy this problem, we propose a new detector by using the magnitude spectra of the received signals.

A. EFFECT OF FREQUENCY-SELECTIVE CHANNELS

Considering the independence between the primary signal and the noise, we can have

$$\mathbf{x}_f(k) \sim \mathcal{CN}\left(\mathbf{0}, N\mathbf{R}_{\mathbf{w}} + \eta N\sigma_s^2 \mathbf{R}_{\mathbf{h}_f}(k)\right). \tag{11}$$

It can be obtained from (11) that the covariance of $\mathbf{x}_f(k)$ is a diagonal matrix under $\mathcal{H}_0$ ($\eta = 0$) but not a diagonal matrix under $\mathcal{H}_1$ ($\eta = 1$). This characteristic can been used for spectrum sensing by detecting whether the population covariance matrix of $\mathbf{x}_f(k)$ is a diagonal matrix or not. This decision is usually made based on the sample covariance matrix, i.e.,

$$\mathbf{R}_{\mathbf{x}_f} = \frac{1}{N}\sum_{k=0}^{N-1}\mathbf{x}_f(k)\mathbf{x}_f^H(k). \tag{12}$$

The expectation of $\mathbf{R}_{\mathbf{x}_f}$ is given by

$$\mathbf{E}[\mathbf{R}_{\mathbf{x}_f}] = N\mathbf{R}_{\mathbf{w}} + \eta\sigma_s^2 \sum_{k=0}^{N-1}\mathbf{R}_{\mathbf{h}_f}(k)$$

$$= N\mathbf{R}_{\mathbf{w}} + \eta\sigma_s^2 \sum_{k=0}^{N-1}\mathbf{h}_f(k)\mathbf{h}_f^H(k). \tag{13}$$

Under flat fading channels, i.e.,

$$h_{t,m}(n) = 0, \quad n \neq 0, \tag{14}$$

the mth element of $\mathbf{h}_f(n)$ is given by

$$h_{f,m}(k) = h_{t,m}(0)e^{-j2\pi\frac{k}{N}\tau_m}. \tag{15}$$

Then, the term $\sum_{n=0}^{N-1}\mathbf{h}_f(k)\mathbf{h}_f^H(k)$ in (13) is a coherent summation if the time delays $\{\tau_m, \forall m\}$ are the same, and the off-diagonal elements of $\mathbf{E}[\mathbf{R}_{\mathbf{x}_f}]$ could have large values.

However, under frequency-selective channels, the term $\sum_{k=0}^{N-1}\mathbf{h}_f(k)\mathbf{h}_f^H(k)$ involves non-coherent summation due to the different phases of $\{\mathbf{h}_f(k), \forall k\}$. Hence, with fixed channel energy, the off-diagonal elements in $\mathbf{E}[\mathbf{R}_{\mathbf{x}_f}]$ have smaller magnitude under frequency-selective channels than under flat fading channels. This may make the off-diagonal elements

of the covariance matrices under $\mathcal{H}_1$ close to zero. Consequently, the difference between the covariance matrices $\mathbf{R}_{\mathbf{x}_f}$ under $\mathcal{H}_0$ and $\mathcal{H}_1$ is reduced in frequency-selective channels. This will induce performance degradation of the covariance matrix based detectors, such as the detector in [19] which exploits spatial correlations.

This problem can be remedied by removing the phase of $\mathbf{h}_f(k)$ to avoid destructive summation, i.e., only the magnitude spectra of channels are used. This leads to a new detector.

B. PROPOSED DETECTOR

To eliminate the negative effect of the phases of $\mathbf{h}_f(n)$ on the summation, we propose to employ the magnitude spectra of the received signals. Denoted by $\mathbf{z}(k) = [z_1(k), \cdots, z_M(k)]^T$ an estimate of the magnitude spectra of the received signals is given by [25], [26]

$$\mathbf{z}(k) = |\mathbf{x}_f(k)|. \tag{16}$$

We then use the covariance matrix of $\mathbf{z}(k)$ rather than $\mathbf{x}_f(k)$ for spectrum sensing. By considering that the mean of $\mathbf{z}(k)$ is nonzero, the covariance matrix of $\mathbf{z}(k)$ is given by [27]

$$\mathbf{R}_{\mathbf{z}} = \frac{1}{N}\sum_{k=0}^{N-1}(\mathbf{z}(k) - \bar{\mathbf{z}})(\mathbf{z}^T(k) - \bar{\mathbf{z}}^T) \tag{17}$$

where

$$\bar{\mathbf{z}} = \frac{1}{N}\sum_{k=0}^{N-1}\mathbf{z}(k). \tag{18}$$

Then the well-known GLRT-based detector under the assumption of a diagonal covariance matrix of noises can be readily employed, which is given by [28], [29]

$$T_{\text{GLRT}} = \frac{\det(\mathbf{R}_{\mathbf{z}})}{\prod\limits_{m=1}^{M}\mathbf{R}_{\mathbf{z}}(m, m)} = \det(\mathbf{C}) \tag{19}$$

where

$$\mathbf{C} = \mathbf{G}\mathbf{R}_{\mathbf{z}}\mathbf{G} \tag{20}$$

with

$$\mathbf{G} = \text{diag}\left\{\frac{1}{\sqrt{\mathbf{R}_{\mathbf{z}}(1, 1)}}, \cdots, \frac{1}{\sqrt{\mathbf{R}_{\mathbf{z}}(M, M)}}\right\}. \tag{21}$$

However, the determinant operation in (19) involves a computational complexity of $\mathcal{O}(M^3)$. To reduce the computational complexity to $\mathcal{O}(M^2)$, we adopt the Frobenius-norm (FN)-based detector as

$$T_{\text{FN}} = ||\mathbf{C}||_F^2 \tag{22}$$

where $||\cdot||_F$ denotes the Frobenius norm. Another reason for adopting the FN-based detector is, as shown in [30], that the FN-based detector is approximately equivalent to the GLRT. With a given decision threshold λ, the decision rule is given by

$$T_{\text{FN}} \underset{\mathcal{H}_0}{\overset{\mathcal{H}_1}{\gtrless}} \lambda. \tag{23}$$

The false-alarm and detection probabilities are, respectively, given by

$$P_f = \text{Prob} \left(T_{\text{FN}} | \mathcal{H}_0 > \lambda \right) \tag{24}$$

and

$$P_d = \text{Prob} \left(T_{\text{FN}} | \mathcal{H}_1 > \lambda \right) \tag{25}$$

where $\text{Prob}(\cdot)$ represents the probability of an event. It is required that $P_f \leq 0.1$ in the first wireless standard based on cognitive radio, e.g., the IEEE 802.22 standard. Higher P_d will decrease the interference to primary users, and in the IEEE 802.22 standard, it is required that $P_d \geq 0.9$.

C. COMPLEXITY ANALYSIS

The computational complexity of the Frobenius-norm operation is $\mathcal{O}(M^2)$. In addition, the computational complexities of fast Fourier transform and obtaining covariance matrix are $\mathcal{O}(MN \log_{10} N)$ and $\mathcal{O}(MN^2)$, respectively. Finally, we can obtain that the computational complexity of the proposed detector is $\mathcal{O}(MN^2)$, which is the same as that of eigenvalue-based and conventional covariance matrix-based detectors.

IV. PERFORMANCE ANALYSIS

A. FALSE-ALARM PROBABILITY

Under $\mathcal{H}_0$, $\mathbf{x}_f(k)$ contains only noise components, and

$$\mathbf{x}_f(k) | \mathcal{H}_0 \sim \mathcal{CN}(\mathbf{0}, N\mathbf{R}_w). \tag{26}$$

It can be obtained that $z_m(k) = |x_{f,m}(k)|$ under $\mathcal{H}_0$ follows Rayleigh distribution, and its mean and variance are

$$\mathbf{E}\left[z_m(k) | \mathcal{H}_0\right] = \frac{\sqrt{N\pi}}{2} \sigma_{w,m} \tag{27}$$

and

$$\mathbf{Var}\left[z_m(k) | \mathcal{H}_0\right] = \frac{N(4-\pi)}{4} \sigma_{w,m}^2, \tag{28}$$

respectively. According to CLT, the mth element of $\bar{\mathbf{z}}$

$$\bar{z}_m | \mathcal{H}_0 = \frac{1}{N} \sum_{k=0}^{N-1} z_m(k) | \mathcal{H}_0, \tag{29}$$

follows a Gaussian distribution, i.e.,

$$\bar{z}_m | \mathcal{H}_0 \sim \mathcal{N}\left(\frac{\sqrt{N\pi}}{2} \sigma_{w,m}, \frac{(4-\pi)}{4} \sigma_{w,m}^2 \right). \tag{30}$$

When $\frac{\sqrt{N\pi}}{2} \sigma_{w,m} \gg \frac{(4-\pi)}{4} \sigma_{w,m}^2$ (i.e., the expectation is far larger than the variance), $\bar{z}_m | \mathcal{H}_0$ can be replaced with its expectation $\frac{\sqrt{N\pi}}{2} \sigma_{w,m}$ [31], i.e.,

$$\bar{z}_m | \mathcal{H}_0 \approx \frac{\sqrt{N\pi}}{2} \sigma_{w,m}, \tag{31}$$

for a sufficiently large N. Similarly, the diagonal elements of $\mathbf{R}_z$ under $\mathcal{H}_0$, i.e., $\mathbf{R}_z(m, m) | \mathcal{H}_0$, $m = 1, \cdots, M$,

can also be approximately replaced by their expectation. Thus

$$\mathbf{R}_z(m, m) | \mathcal{H}_0 \approx \mathbf{E}\left[\mathbf{R}_z(m, m) | \mathcal{H}_0\right]$$

$$= \mathbf{E}\left[\frac{1}{N} \sum_{k=0}^{N-1} (z_m(k) - \bar{z}_m)^2 | \mathcal{H}_0 \right]$$

$$= \frac{1}{N} \sum_{k=0}^{N-1} \mathbf{E}\left[(z_m(k) - \bar{z}_m)^2 | \mathcal{H}_0 \right]$$

$$\approx \frac{1}{N} \sum_{k=0}^{N-1} \mathbf{E}\left[\left(z_m(k) - \frac{\sqrt{N\pi}}{2} \sigma_{w,m} \right)^2 | \mathcal{H}_0 \right]$$

$$= \frac{N(4-\pi)}{4} \sigma_{w,m}^2. \tag{32}$$

For the off-diagonal elements of $\mathbf{R}_z$, according to CLT, we have

$$\mathbf{R}_z(p, q) | \mathcal{H}_0 = \frac{1}{N} \sum_{k=0}^{N-1} \left(z_p(k) - \bar{z}_p \right) \left(z_q(k) - \bar{z}_q \right) | \mathcal{H}_0$$

$$\sim \mathcal{N}\left(0, \frac{1}{N} \left(\frac{N(4-\pi)}{4} \right)^2 \sigma_{w,p}^2 \sigma_{w,q}^2 \right) \tag{33}$$

where $p \neq q$. Thus,

$$\mathbf{C}(p, q) | \mathcal{H}_0 = \frac{\mathbf{R}_z(p, q) | \mathcal{H}_0}{\sqrt{\mathbf{R}_z(p, p) | \mathcal{H}_0} \sqrt{\mathbf{R}_z(q, q) | \mathcal{H}_0}}$$

$$\approx \frac{\mathbf{R}_z(p, q) | \mathcal{H}_0}{\frac{N(4-\pi)}{4} \sqrt{\sigma_{w,p}^2 \sigma_{w,q}^2}}. \tag{34}$$

Combining (33) and (34) yields

$$\mathbf{C}(p, q) | \mathcal{H}_0 \sim \mathcal{N}\left(0, \frac{1}{N} \right), \quad p \neq q. \tag{35}$$

It can be easily verified that the elements of $\{\mathbf{C}(p, q), p > q\}$ are independent of each other under $\mathcal{H}_0$. In addition, $\mathbf{C}$ is a symmetric matrix with all diagonal elements being one. Therefore, the test-statistic in (22) under $\mathcal{H}_0$ can be rewritten as

$$T_{\text{FN}} | \mathcal{H}_0 = M + \frac{2}{N} \chi_K^2 \tag{36}$$

where $K = (M^2 - M)/2$ and χ_K^2 represents a central chi-square distribution with degree-of-freedom of K. Thus, for a decision threshold λ, the false alarm probability P_f is given by

$$P_f = \int_{\frac{(\lambda - M)N}{2}}^{+\infty} f_{\chi_K^2}(z) dz \tag{37}$$

where $f_{\chi_K^2}(\cdot)$ denotes the probability density function (PDF) of χ_K^2.

B. DETECTION PROBABILITY

Proposition 1: $\mathbf{C}(p, q)$ under $\mathcal{H}_1$ for $p \neq q$ approximately follows a Gaussian distribution as

$$\mathbf{C}(p, q)|\mathcal{H}_1 \sim \mathcal{N}\left(\mu_{p,q}, \sigma_{p,q}^2\right), \quad p \neq q \qquad (38)$$

where $\mu_{p,q}$ and $\sigma_{p,q}^2$ are give in (A.14) and (A.15) of Appendix A.

Proof: See Appendix A. ∎

With **Proposition 1**, the test-statistic T_{FN} under $\mathcal{H}_1$ can be approximately given by

$$T_{\text{FN}}|\mathcal{H}_1 = M + 2\bar{\sigma}^2 \chi_K^2(\gamma) \qquad (39)$$

where

$$\bar{\sigma}^2 = \frac{\sum_{p>q} \sigma_{p,q}^2}{(M^2 - M)/2} \qquad (40)$$

and $\chi_K^2(\gamma)$ denotes a noncentral chi-square distribution with degree-of-freedom of K and

$$\gamma = \sum_{p>q} \left(\frac{\mu_{p,q}}{\sigma_{p,q}}\right)^2. \qquad (41)$$

Thus, for a decision threshold λ, the detection probability P_d is given by

$$P_d = \int_{\frac{(\lambda-M)N}{2}}^{+\infty} f_{\chi_K^2(\lambda)}(z) dz \qquad (42)$$

where $f_{\chi_K^2(\lambda)}(\cdot)$ denotes the PDF of $\chi_K^2(\lambda)$.

V. SIMULATION RESULTS

In this section, we verify the theoretical analyses and evaluate the performance of the proposed detector through numerical simulations. In the simulations, the average channel energies are assumed to be one, i.e., $\sum_{l=0}^{L-1} \mathbf{E}[|h_m(l)|^2] = 1, \forall m$, where L denotes the channel length. The channel coefficients $\{h_m(l), \forall m, l\}$ are assumed to be complex Gaussian distributed in the simulation, i.e., we employ the Rayleigh channel. It should be noticed that the proposed detector also works for other fading channels. SNR in dB is defined as

$$\text{SNR} = 10 \log_{10}\left(\frac{\sigma_s^2}{\frac{1}{M}\sum_{m=1}^{M} \sigma_{w,m}^2}\right). \qquad (43)$$

Fig. 1 shows the theoretical and Monte Carlo results for the false-alarm and detection probabilities of the proposed detectors, when $M = 4$, $N = 256$ and $L = 40$. In each Monte Carlo trial, the noise powers $\sigma_{w,m}^2, \forall m$, are randomly generated from a uniform distribution before their average is normalized. It can be observed from Fig. 1 that the analytical result for P_f matches the corresponding Monte Carlo result very well. Hence, it can be effectively used for setting the decision threshold for a target P_f. In addition, the analytical result for P_d, which can be used for evaluating the detection
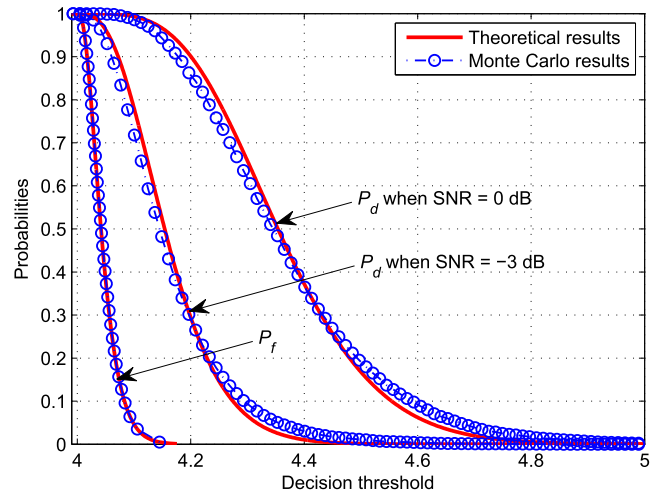

FIGURE 1. Theoretical and Monte Carlo results for false-alarm and detection probabilities when $M = 4$.

performance of the proposed detector, matches the corresponding Monte Carlo result. By increasing M from 4 to 8, while keeping other parameters unchanged, Fig. 2 shows the theoretical and Monte Carlo results for the false-alarm and detection probabilities of the proposed detector. It again demonstrates that our theoretical results match the Monte Carlo results.
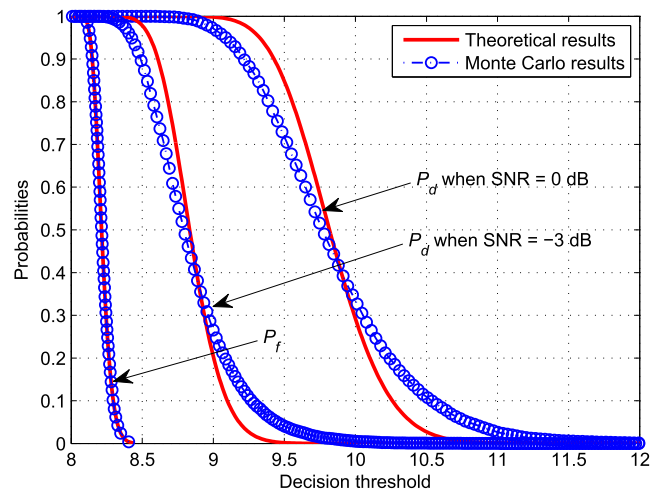

FIGURE 2. Theoretical and Monte Carlo results for false-alarm and detection probabilities when $M = 8$.

Fig. 3 shows the detection probabilities of various detectors for different SNRs when the receiver is calibrated, i.e., the detection probabilities are obtained when the noise powers among antennas are identical. The other parameter settings are $M = 4$, $N = 256$, $L = 40$ and $P_f = 0.1$. The performances of ED with noise uncertainty (UN) of 0.25dB and 0.5dB are also presented. It can be observed from Fig. 3 that the proposed detector delivers the best performance. Specifically, to achieve a detection probability of 0.9, the proposed detector requires lower SNR than the other detectors by at least 1.4 dB.
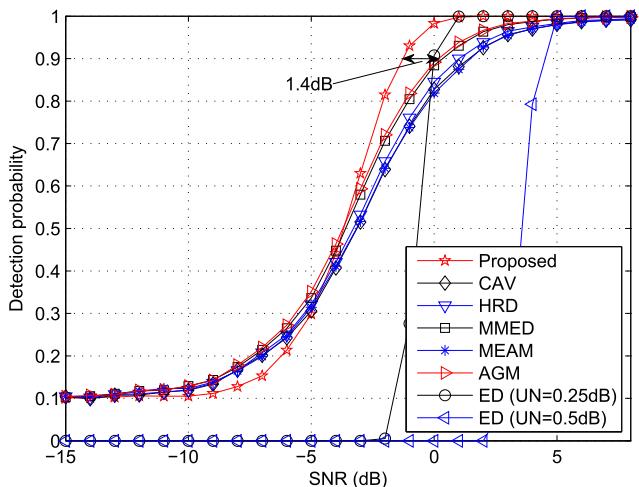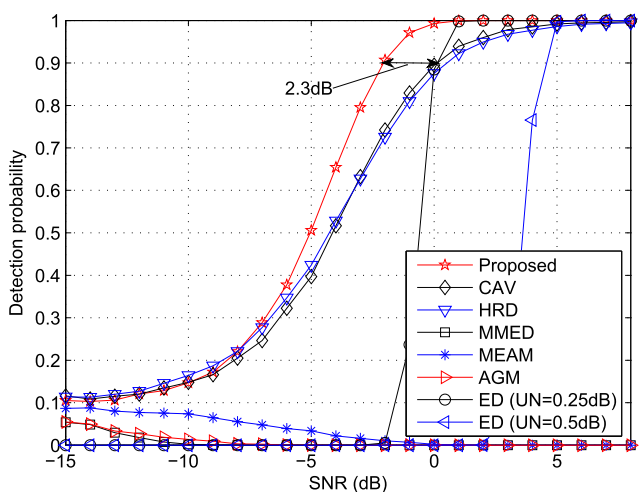
FIGURE 3. P_d versus SNR with calibrated receiver.

FIGURE 4. P_d versus SNR with uncalibrated receiver.

FIGURE 5. P_d versus channel length L with calibrated receiver.
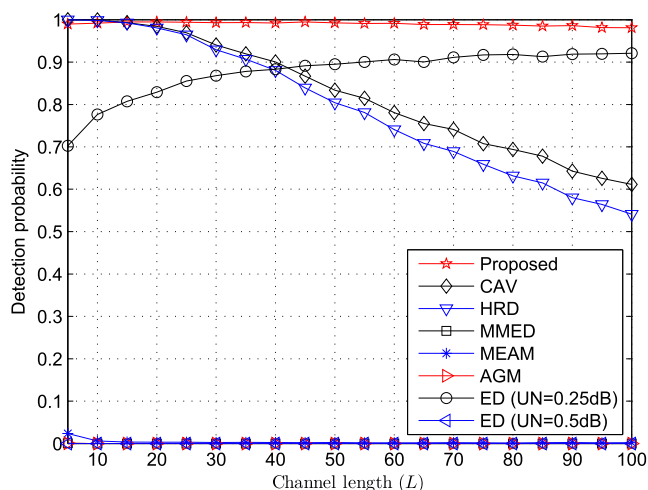
FIGURE 6. P_d versus channel length L with uncalibrated receiver.
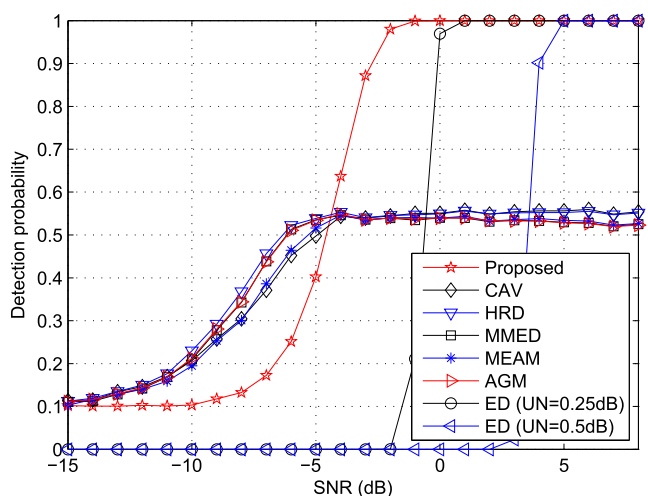
FIGURE 7. P_d versus SNR with calibrated receiver with different time delays.

For the case without calibrating receiver (i.e., the antennas have different noise powers), Fig. 4 shows the detection probabilities of these detectors for different SNRs. It can be observed that eigenvalue-based detectors (MMED, MEAM and AGM) fail in spectrum sensing. The proposed detector still has the best performance among these detectors. To achieve a detection probability of 0.9, the proposed detector requires lower SNR than the other detectors by at least 2.3 dB.

Fig. 5 shows the detection probabilities of various detectors versus channel length L when the receiver is calibrated. The parameter settings are $M = 4$, $N = 256$, SNR $= 0$ dB and $P_f = 0.1$. Here, we set the channel length up to 100, as in some practice scenarios, the channel length may be up to hundreds of taps such as in digital television (DTV) applications [33]. It is observed from Fig. 5 that the detection probability of the proposed detector keeps high for different channel lengths, while the detection probabilities of other detectors degrade significantly with the increase of channel length.
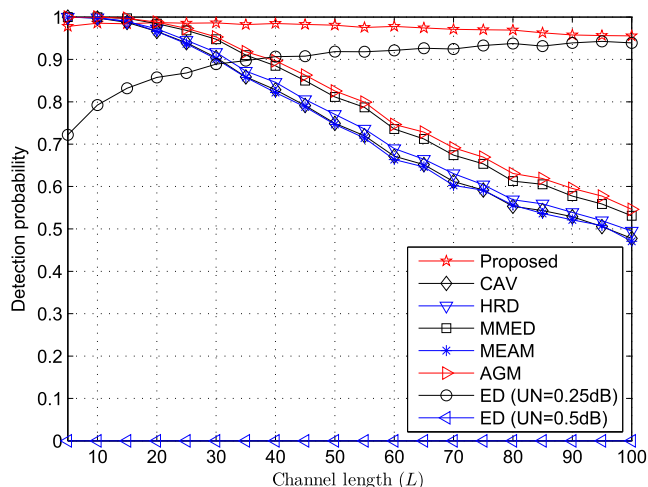
Fig. 6 shows the detection probabilities of various detectors versus channel length L when the receiver is not calibrated. The parameter settings are $M = 4$, $N = 256$, SNR $= 0$ dB

FIGURE 8. P_d versus SNR with uncalibrated receiver with different time delays.

and $P_f = 0.1$. It is observed from Fig. 6 that the detection probability of the proposed detector keeps high for different channel lengths, while the detection probabilities of other detectors degrade significantly with the 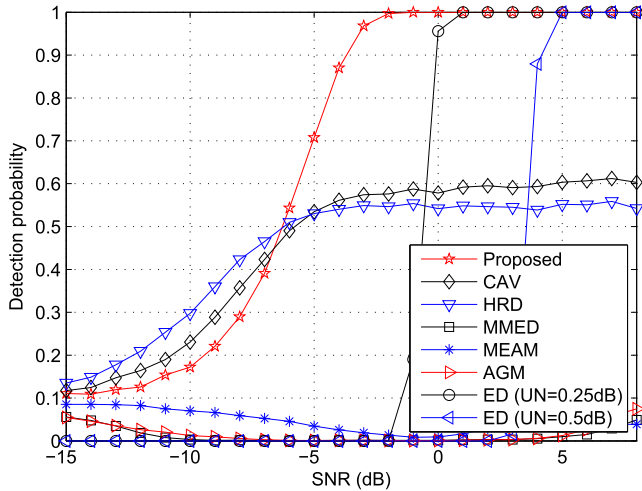increase of channel length. Fig. 6 shows again that the eigenvalue-based detectors (MMED, MEAM and AGM) fail in spectrum sensing because of the nonidentical noise powers.

In the following, we investigate the effect of time delays τ_m on the performance of the detectors. We assume that the time delays are uniformly distributed between 1 and 10. Fig. 7 shows the detection probabilities of various detectors for different SNRs when the receiver is calibrated, and Fig. 8 when the receiver is not calibrated. It can be observed that the proposed detector can achieve a detection probability of one when SNR increases, while the other detectors cannot. This is because different time delays degrade the correlation of received signals among antennas.

VI. CONCLUSION

In this work, we have investigated the effect of multipath propagation on covariance matrix based spectrum sensing. To eliminated the negative impact of the phases of channel spectra on the covariance matrix of received signals, we have proposed a new detector which exploits the magnitude spectra of the received signals only. The false-alarm and detection probabilities of the proposed detector have been derived. Simulation results have been provided, which validate the theoretical analyses and demonstrate the superior performance of the proposed detector.

APPENDIX A
PROOF OF PROPOSITION 1

Under $\mathcal{H}_1$, we have

$$\mathbf{x}_f(k)|\mathcal{H}_1 \sim \mathcal{CN}\left(\mathbf{0}, N\mathbf{R_w} + N\sigma_s^2\mathbf{R_{h_f}}(k)\right). \quad (A.1)$$

It can be obtained from (5) that the elements of $\mathbf{x}_f(k)|\mathcal{H}_1$ at different k are independent of each other, as $s_f(n)$ and $\mathbf{w}_f(k)$ are independent for different k. It can also be obtained that $z_m(k) = |x_{f,m}(k)|$ under $\mathcal{H}_1$ follows a Rayleigh distribution, and its mean and variance are

$$\mathbf{E}\left[z_m(k)|\mathcal{H}_1\right] = \frac{\sqrt{N\pi}}{2} \times \sqrt{\sigma_{w,m}^2 + \sigma_s^2|h_{f,m}(k)|^2} \quad (A.2)$$

and

$$\mathbf{Var}\left[z_m(k)|\mathcal{H}_1\right] = \frac{N(4-\pi)}{4} \times \left(\sigma_{w,m}^2 + \sigma_s^2|h_{f,m}(k)|^2\right), \quad (A.3)$$

respectively. For a sufficiently large N, we can obtain that $\bar{z}_m$ under $\mathcal{H}_1$ approximately equals to its expectation, i.e.,

$$\bar{z}_m|\mathcal{H}_1 \approx \frac{\sqrt{N\pi}}{2} \times \frac{1}{N}\sum_{n=0}^{N-1}\sqrt{\sigma_{w,m}^2 + \sigma_s^2|h_{f,m}(k)|^2}. \quad (A.4)$$

Considering that, with a sufficiently large N, $\mathbf{R_z}(m,m)|\mathcal{H}_1$ can be approximately replaced by its expectation [31], we have

$$\mathbf{R_z}(m,m)|\mathcal{H}_1 \approx \mathbf{E}\left[\mathbf{R_z}(m,m)|\mathcal{H}_1\right]$$
$$= \mathbf{E}\left[\frac{1}{N}\sum_{k=0}^{N-1}(z_m(k) - \bar{z}_m)^2 |\mathcal{H}_1\right]$$
$$= \frac{N(4-\pi)}{4}\left(\sigma_{w,m}^2 + \frac{\sigma_{s,m}^2}{N}\sum_{k=0}^{N-1}|h_{f,m}(k)|^2\right)$$
$$+ \frac{\pi}{4}\sum_{k=0}^{N-1}\left(\sqrt{\sigma_{w,m}^2 + \sigma_s^2|h_{f,m}(k)|^2}\right.$$
$$\left. - \frac{1}{N}\sum_{l=0}^{N-1}\sqrt{\sigma_{w,m}^2 + \sigma_s^2|h_{f,m}(l)|^2}\right)^2. \quad (A.5)$$

In addition, for $p \neq q$,

$$\mathbf{R_z}(p,q)|\mathcal{H}_1 = \frac{1}{N}\sum_{k=0}^{N-1}\left(z_p(k) - \bar{z}_p\right)\left(z_q(k) - \bar{z}_q\right)|\mathcal{H}_1$$
$$= \frac{1}{N}\sum_{k=0}^{N-1}z_q(k)z_q(k) - \bar{z}_p\bar{z}_q|\mathcal{H}_1$$
$$= \frac{1}{N}\sum_{k=0}^{N-1}|x_{f,p}(k)x_{f,q}(k)| - \bar{z}_p\bar{z}_q|\mathcal{H}_1. \quad (A.6)$$

From (A.1), the correlation coefficient between $x_{f,p}(k)$ and $x_{f,q}(k)$ is given by

$$\rho_{p,g}(k) = \frac{\sigma_s^2|h_{f,p}(k)h_{f,q}(k)|}{\sqrt{\left(\sigma_{w,p}^2 + \sigma_s^2|h_{f,p}(k)|^2\right)\left(\sigma_{w,q}^2 + \sigma_s^2|h_{f,q}(k)|^2\right)}}. \quad (A.7)$$

Hence, the mean and variance of $|x_{f,p}(k)x_{f,q}(k)|$ are respectively given by [32]

$$
\mathbf{E}\left[|x_{f,p}(k)x_{f,q}(k)|\right] = 2N\sigma_s^2|h_{f,p}(k)h_{f,q}(k)|\left(1-\rho_{p,g}^2(k)\right)^3
$$
$$
\times \frac{\Gamma^2(1.5)}{\Gamma^2(0.5)}\,_2F_1(1.5, 1.5, 1, \rho_{p,g}^2(k)) \quad \text{(A.8)}
$$

and

$$
\mathbf{Var}\left[|x_{f,p}(k)x_{f,q}(k)|\right]
$$
$$
= 4N^2\sigma_s^4|h_{f,p}(k)h_{f,q}(k)|^2\left(1-\rho_{p,g}^2(k)\right)^4\frac{\Gamma^2(2)}{\Gamma^2(0.5)}
$$
$$
\times\,_2F_1(2, 2, 1, \rho_{p,g}^2(k)) - \mathbf{E}^2\left[|x_{f,p}(k)x_{f,q}(k)|\right] \quad \text{(A.9)}
$$

where $\Gamma(\cdot)$ denotes the Gamma function and $_2F_1(\cdot, \cdot, \cdot, \cdot)$ denotes the hypergeometric function.

Therefore, according to CLT, $\mathbf{R_z}(p, q)|\mathcal{H}_1$ in (A.6) approximately follows a Gaussian distribution with mean

$$
\mathbf{E}\left[\mathbf{R_z}(p, q)|\mathcal{H}_1\right] = \frac{1}{N}\sum_{k=0}^{N-1}\mathbf{E}\left[|x_{f,p}(k)x_{f,q}(k)|\right]
$$
$$
- \frac{N\pi}{4}\left(\frac{1}{N}\sum_{k=0}^{N-1}\sqrt{\sigma_{w,p}^2 + \sigma_s^2|h_{f,p}(k)|^2}\right)
$$
$$
\times\left(\frac{1}{N}\sum_{k=0}^{N-1}\sqrt{\sigma_{w,q}^2 + \sigma_s^2|h_{f,q}(k)|^2}\right)
$$
$$
\text{(A.10)}
$$

and variance

$$
\mathbf{Var}\left[\mathbf{R_z}(p, q)|\mathcal{H}_1\right] = \frac{1}{N^2}\sum_{n=0}^{N-1}\mathbf{Var}\left[|x_{f,p}(k)x_{f,q}(k)|\right]. \quad \text{(A.11)}
$$

Hence,

$$
\mathbf{C}(p, q)|\mathcal{H}_1 = \frac{\mathbf{R_z}(p, q)|\mathcal{H}_1}{\sqrt{\mathbf{R_z}(p, p)|\mathcal{H}_1}\sqrt{\mathbf{R_z}(q, q)|\mathcal{H}_1}} \quad \text{(A.12)}
$$

follows a Gaussian distribution. Let

$$
\mathbf{C}(p, q)|\mathcal{H}_1 \sim \mathcal{N}\left(\mu_{p,q}, \sigma_{p,q}^2\right), \quad p \neq q \quad \text{(A.13)}
$$

where $\mu_{p,q}$ and $\sigma_{p,q}^2$ denote the expectation and variance of $\mathbf{C}(p, q)|\mathcal{H}_1$, respectively, i.e.,

$$
\mu_{p,q} = \frac{\mathbf{E}\left[\mathbf{R_z}(p, q)|\mathcal{H}_1\right]}{\sqrt{\mathbf{R_z}(p, p)|\mathcal{H}_1}\sqrt{\mathbf{R_z}(q, q)|\mathcal{H}_1}}, \quad \text{(A.14)}
$$
$$
\sigma_{p,q}^2 = \frac{\mathbf{Var}\left[\mathbf{R_z}(p, q)|\mathcal{H}_1\right]}{\mathbf{R_z}(p, p)|\mathcal{H}_1\mathbf{R_z}(q, q)|\mathcal{H}_1}. \quad \text{(A.15)}
$$

■

REFERENCES

[1] S. Haykin, "Cognitive radio: Brain-empowered wireless communications," *IEEE J. Sel. Areas Commun.*, vol. 23, no. 2, pp. 201–220, Feb. 2005.

[2] I. F. Akyildiz, W.-Y. Lee, M. C. Vuran, and S. Mohanty, "A survey on spectrum management in cognitive radio networks," *IEEE Commun. Mag.*, vol. 46, no. 4, pp. 40–48, Apr. 2008.

[3] T. Yucek and H. Arslan, "A survey of spectrum sensing algorithms for cognitive radio applications," *IEEE Commun. Surveys Tuts.*, vol. 11, no. 1, pp. 116–130, 1st Quart., 2009.

[4] A. Ali and W. Hamouda, "Advances on spectrum sensing for cognitive radio networks: Theory and applications," *IEEE Commun. Surveys Tuts.*, vol. 19, no. 2, pp. 1277–1304, 2nd Quart., 2016.

[5] A. Sonnenschein and P. M. Fishman, "Radiometric detection of spread-spectrum signals in noise of uncertain power," *IEEE Trans. Aerosp. Electron. Syst.*, vol. 28, no. 3, pp. 654–660, Jul. 1992.

[6] A. Mariani, A. Giorgetti, and M. Chiani, "Effects of noise power estimation on energy detection for cognitive radio applications," *IEEE Trans. Commun.*, vol. 59, no. 12, pp. 3410–3420, Dec. 2011.

[7] V. Rakovic, D. Denkovski, V. Atanasovski, P. Mähönen, and L. Gavrilovska, "Capacity-aware cooperative spectrum sensing based on noise power estimation," *IEEE Trans. Commun.*, vol. 63, no. 7, pp. 2428–2441, Jul. 2015.

[8] M. Jin, Q. Guo, J. Tong, J. Xi, and Y. Li, "Energy detection of DVB-T signals against noise uncertainty," *IEEE Commun. Lett.*, vol. 18, no. 10, pp. 1831–1834, Oct. 2014.

[9] M. Jin, Q. Guo, J. Xi, Y. Li, and Y. Li, "On spectrum sensing of OFDM signals at low SNR: New detectors and asymptotic performance," *IEEE Trans. Signal Process.*, vol. 65, no. 12, pp. 3218–3233, Jun. 2017.

[10] P. Urriza, E. Rebeiz, and D. Cabric, "Multiple antenna cyclostationary spectrum sensing based on the cyclic correlation significance test," *IEEE J. Sel. Areas Commun.*, vol. 31, no. 11, pp. 2185–2195, Nov. 2013.

[11] A. Kortun, T. Ratnarajah, M. Sellathurai, Y.-C. Liang, and Y. Zeng, "On the eigenvalue-based spectrum sensing and secondary user throughput," *IEEE Trans. Veh. Technol.*, vol. 63, no. 3, pp. 1480–1486, Mar. 2014.

[12] A. Taherpour, M. Nasiri-Kenari, and S. Gazor, "Multiple antenna spectrum sensing in cognitive radios," *IEEE Trans. Wireless Commun.*, vol. 9, no. 2, pp. 814–823, Feb. 2010.

[13] J. Sala-Alvarez, G. Vázquez-Vilar, R. López-Valcarce, S. Sedighi, and A. Taherpour, "Multiantenna GLR detection of rank-one signals with known power spectral shape under spatially uncorrelated noise," *IEEE Trans. Signal Process.*, vol. 64, no. 23, pp. 6269–6283, Dec. 2016.

[14] D. Ramirez, G. Vázquez-Vilar, R. López-Valcarce, J. Via, and I. Santamaria, "Detection of rank-*P* signals in cognitive radio networks with uncalibrated multiple antennas," *IEEE Trans. Signal Process.*, vol. 59, no. 8, pp. 3764–3774, Aug. 2011.

[15] Y. Zeng and Y.-C. Liang, "Spectrum-sensing algorithms for cognitive radio based on statistical covariances," *IEEE Trans. Veh. Technol.*, vol. 58, no. 4, pp. 1804–1815, May 2009.

[16] M. Jin, Y. Li, and H.-G. Ryu, "On the performance of covariance based spectrum sensing for cognitive radio," *IEEE Trans. Signal Process.*, vol. 60, no. 7, pp. 3670–3682, Jul. 2012.

[17] M. Jin, Q. Guo, J. Xi, Y. Li, Y. Yu, and D. D. Huang, "Spectrum sensing using weighted covariance matrix in Rayleigh fading channels," *IEEE Trans. Veh. Technol.*, vol. 64, no. 11, pp. 5137–5148, Nov. 2015.

[18] Z. Pourgharehkhan, A. Taherpour, J. Sala-Alvarez, and T. Khattab, "Correlated multiple antennas spectrum sensing under calibration uncertainty," *IEEE Trans. Wireless Commun.*, vol. 14, no. 12, pp. 6777–6791, Dec. 2015.

[19] J. K. Tugnait, "On multiple antenna spectrum sensing under noise variance uncertainty and flat fading," *IEEE Trans. Signal Process.*, vol. 60, no. 4, pp. 1823–1832, Apr. 2012.

[20] P. Wang, J. Fang, N. Han, and H. Li, "Multiantenna-assisted spectrum sensing for cognitive radio," *IEEE Trans. Veh. Technol.*, vol. 59, no. 4, pp. 1791–1880, May 2010.

[21] R. Zhang, T. J. Lim, Y.-C. Liang, and Y. Zeng, "Multi-antenna based spectrum sensing for cognitive radios: A GLRT approach," *IEEE Trans. Commun.*, vol. 58, no. 1, pp. 84–88, Jan. 2010.

[22] L. Wei and O. Tirkkonen, "Spectrum sensing in the presence of multiple primary users," *IEEE Trans. Commun.*, vol. 60, no. 5, pp. 1268–1277, May 2012.

[23] A. Conti, M. Z. Win, and M. Chiani, "Slow adaptive *M*-QAM with diversity in fast fading and shadowing," *IEEE Trans. Commun.*, vol. 55, no. 5, pp. 895–905, May 2007.

[24] S. Dikmese, P. C. Sofotasios, M. Renfors, and M. Valkama, "Subband energy based reduced complexity spectrum sensing under noise uncertainty and frequency-selective spectral characteristics," *IEEE Trans. Signal Process.*, vol. 64, no. 1, pp. 131–145, Jan. 2016.

[25] X. Zhu, G. T. Beauregard, and L. L. Wyse, "Real-time signal estimation from modified short-time Fourier transform magnitude spectra," *IEEE Trans. Audio, Speech, Language Process.*, vol. 15, no. 5, pp. 1645–1653, Jul. 2007.

[26] P. C. Loizou, "Speech enhancement based on perceptually motivated Bayesian estimators of the magnitude spectrum," *IEEE Trans. Speech Audio Process.*, vol. 13, no. 5, pp. 857–869, Sep. 2005.

[27] J. P. Hoffbeck and D. A. Landgrebe, "Covariance matrix estimation and classification with limited training data," *IEEE Trans. Pattern Anal. Mach. Intell.*, vol. 18, no. 7, pp. 763–767, Jul. 1996.

[28] L. Huang, Y. Xiao, H. C. So, and J. Fang, "Accurate performance analysis of Hadamard ratio test for robust spectrum sensing," *IEEE Trans. Wireless Commun.*, vol. 14, no. 2, pp. 750–758, Feb. 2015.

[29] S. Sedighi, A. Taherpour, J. Sala-Alvarez, and T. Khattab, "On the performance of Hadamard ratio detector-based spectrum sensing for cognitive radios," *IEEE Trans. Signal Process.*, vol. 63, no. 14, pp. 3809–3824, Jul. 2015.

[30] D. E. Hack, C. W. Rossler, and L. K. Patton, "Multichannel detection of an unknown rank-N signal using uncalibrated receivers," *IEEE Signal Process. Lett.*, vol. 21, no. 8, pp. 998–1002, Aug. 2014.

[31] V. Upadhya and D. Jalihal, "Almost exact threshold calculations for covariance absolute value detection algorithm," in *Proc. Nat. Conf. Commun. (NCC)*, Feb. 2012, pp. 1–5.

[32] M. K. Simon, *Probability Distributions Involving Gaussian Random Variables: A Handbook for Engineers and Scientists*. New York, NY, USA: Springer, 2002.

[33] I. Garrison *et al.*, "DTV channel characterization," in *Proc. Conf. Inf. Sci. Syst.*, 2001, pp. 1–6.

QINGHUA GUO (S'07–M'08) received the B.E. degree in electronic engineering and the M.E. degree in signal and information processing from Xidian University, Xi'an, China, in 2001 and 2004, respectively, and the Ph.D. degree in electronic engineering from the City University of Hong Kong, Hong Kong, in 2008.

He is currently a Senior Lecturer with the School of Electrical, Computer and Telecommunications Engineering, University of Wollongong, Wollongong, NSW, Australia, and an Adjunct Associate Professor with the School of Electrical, Electronic and Computer Engineering, The University of Western Australia, Perth, WA, Australia. His research interests include signal processing and telecommunication. He was a recipient of the Australian Research Council's Discovery Early Career Researcher Award.

YOUMING LI received the B.S. degree in computational mathematics from Lanzhou University, Lanzhou, China, in 1985, the M.S. degree in computational mathematics from Xi'an Jiaotong University, Xi'an, China, in 1988, and the Ph.D. degree in electrical engineering from Xidian University, Xi'an, in 1995. From 1988 to 1998, he was with the Department of Applied Mathematics, Xidian University, where he was an Associate Professor. From 1999 to 2000, he was a Research Fellow with the School of EEE, Nanyang Technological University, Singapore. From 2001 to 2003, he joined DSO National Laboratories, Singapore. In 2004, he was a Research Fellow with the School of Engineering, Bar-Ilan University, Israel. Since 2005, he has been with the Faculty of Electrical Engineering and Computer Science, Ningbo University, where he is currently a Vice Dean and a Professor. His research interests are in the areas of statistical signal processing and its application in communications, cognitive radio, and underwater acoustic communication.

• • •

MING JIN received the B.E. and Ph.D. degrees in electrical engineering from Xidian University, Xi'an, China, in 2005 and 2010, respectively. From 2013 to 2014, he was an Associate Researcher with the School of Electrical, Computer and Telecommunications Engineering, University of Wollongong, Wollongong, NSW, Australia. He is currently an Associate Professor with the Faculty of Electrical Engineering and Computer Science, Ningbo University, Ningbo, China. His current research interests include spectrum sensing and channel estimation.